Geochemistry International, Vol. 41, No. 8, 2003, pp. 770–786. Translated from Geokhimiya, No. 8, 2003, pp. 847–865.

Burakovo–Aganozero Layered Massif of the Trans-Onega Region: 1. Geochemical Structure of the Layered Series

G. S. Nikolaev* and D. M. Khvorov**

**Vernadsky Institute of Geochemistry and Analytical Chemistry, Russian Academy of Sciences, ul. Kosygina 19, Moscow, 119991 Russia*
e-mail: gsnik@geokhi.ru

*** Faculty of Geology, Moscow State University, Vorob'evy gory, Moscow, 119899 Russia*
e-mail: dhvorov@mail.ru

Received December 16, 2001

Abstract—The paper presents an examination and interpretation of petrogeochemical data on the basis of the phase composition of cumulates. A new structural scheme of the Layered Series of the massif is proposed. The Layered Series shows an upsection change of zones of olivine, two-pyroxene, two-pyroxene–plagioclase, and magnetite–two-pyroxene–plagioclase cumulates. This change corresponds to the succession of the typomorphic cumulus assemblages, which, in the first approximation, can be taken as the crystallization order of primary magma. It was demonstrated that the rocks formed simultaneously in different parts of the magmatic chamber with diverse geochemical features determined by different porosities of cumulus frameworks. The zone of two-pyroxene cumulates is complicated by a peridotite horizon and a leucogabbro–anorthosite layer, with the former produced by injection of a new magma portion. The spatial relation of leucogabbros and anorthosites to the rocks affected by the strongest subsolidus alteration (monomineral clinopyroxenites) suggests that they crystallized within one chamber.

STATE OF THE PROBLEM AND GOALS OF INVESTIGATION

The Early Proterozoic Burakovo–Aganozer intrusion is located in the Eastern Onega region within the Vodlozero block of the Karelian granite–greenstone terrane in the central part of the Burakovo–Monastyr permeable zone and intrudes the Early Archean tonalite–amphibolite complexes and Late Archean gneissic granites [1]. This is the largest layered intrusion in Europe more than 630 km^2 in area on the present-day erosion level. The massif is nearly completely overlain by thick Quaternary deposits.

In plan, it forms a NE-trending body (Fig. 1). The NW-trending faults divide the massif into three blocks: Burakovo (southwestern), Shalozero (central), and Aganozero (northeastern). Geological–geophysical investigations [2, 3] showed that the intrusion is lopolithic in shape and can be subdivided into two segments: a trough-shaped one consisting of the Burakovo and Shalozero blocks, and the funnel-shaped Aganozero block. The gravimetrically deduced map of the massif floor relief is shown in Fig. 1 (inset). The maximum bottom depth of the intrusion is observed in the funnel-shaped Aganozero block with a thickness of >8 km. The floor of the trough-shaped part of the massif is as deep as 7.5 km in the Burakovo block and 6.5 km in the Shalozero block. Geological–geophysical data [4] indicate sharp contacts of the massif with host rocks, with steeper southern and southeastern contacts (45°–70°) and gentler northern and northwestern ones (40°–45°).

The massif hosts chromite [5, 6] and nickel silicate [7] deposits and could potentially contain an economic-grade platinum mineralization [8–10]. Moreover, the problem of emplacement of such a large intrusion and formation of its geochemical structure is of great theoretical interest. Because of this, it has attracted significant attention of geologists and was considered in numerous publications.

The intrusion is composed of the predominant Layered Series and Border Group. For understanding the vertical structure of the Burakovo–Aganozero Massif, it is very important to construct a scheme of the Layered Series stratification. However, it is a difficult task, since the massif is nearly unexposed and its structure can be revealed only by drilling material of 300 unevenly distributed boreholes. Three different approaches exist for deciphering the stratification of this layered intrusion.

Based on a traditional petrographic study, Lavrov [9, 11] proposed the following scheme of stratigraphy (from bottom to top): *an ultramafic* zone with lower *dunite* (>3000 m thick) and upper *peridotite* (about 400 m) subzones; *a transitional* zone (400 m) consisting of two lherzolite–wehrlite–pyroxenite–gabbronorite–anorthosite megarhythms; *a gabbronorite* zone with *lower* (650 m), *middle* (750 m), and *upper* (500 m) subzones; and *a magnetite gabbronorite* zone (600 m).

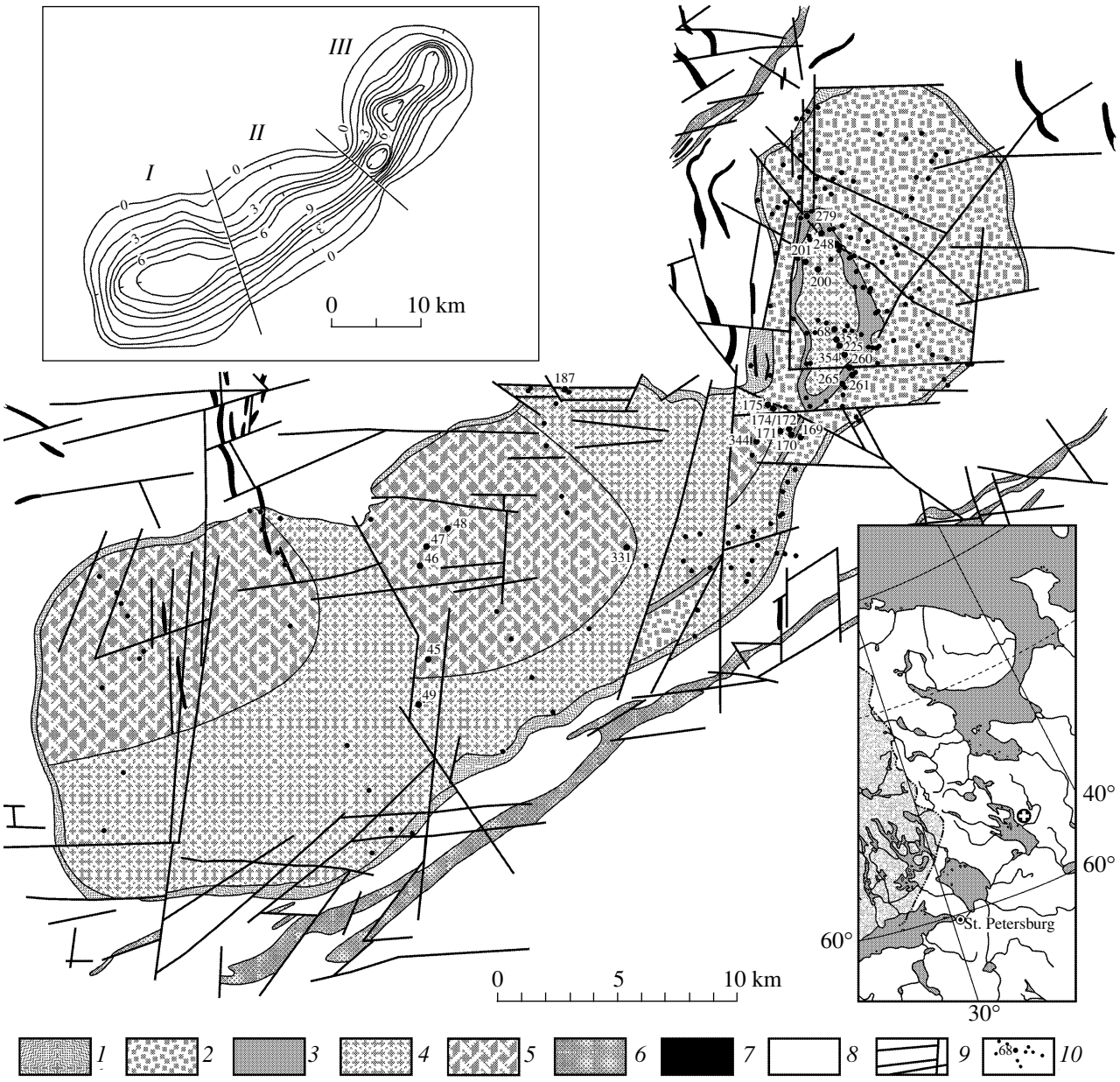

Fig. 1. Geological scheme of the Burakovo–Aganozero layered pluton modified after [13, 31]. Rocks of the pluton: (*1*) Border Group; Layered Series: (*2*) zone of olivine cumulates; (*3*) zone of two-pyroxene cumulates; (*4*) zone of two-pyroxene–plagioclase cumulates; (*5*) zone of magnetite–two-pyroxene–plagioclase cumulates. Dike complexes: (*6*) Koplozero–Avdeev ultramafic–mafic; (*7*) Pudozhgorsk gabbroid; (*8*) Archean–Proterozoic host rocks; (*9*) faults; (*10*) boreholes with numbers; the inset below shows the location of the pluton (cross); the inset above shows the relief of the magmatic chamber floor after [2], the contour interval is 1 kilometer. The Roman numerals denote blocks: (*I*) Burakovo, (*II*) Shalozero, (*III*) Aganozero.

Another approach to the stratification of the Layered Series of the massif was proposed by Koptev-Dvornikov [12–14]. Following the traditional investigations of layered massifs [15], zones were distinguished on the basis of cumulus assemblages, which imparted genetic sense to stratigraphic subdivisions. The boundaries between zones were determined not on the basis of change of petrographic rock type, but by the appearance of a typomorphic cumulus assemblage. In addition, these investigations mark a fundamentally new step in the correlation of the borehole sections. Stratification earlier based only on petrographic study was performed using easily formalizable petrochemical data. Five zones were distinguished in the Layered Series: *an ultramafic* zone (3000–3500 m thick) with a lower *dunite* subzone and an upper *poikilitic gabbro–peridotite* subzone (about 400 m); *a pyroxenite* zone (100–200 m); *a gabbronorite* zone with *lower* (banded)

(450 m) and *upper* (650 m) subzones; a zone of *gabbronorite with inverted pigeonite* (1150 m); and a *magnetite gabbronorite–diorite* zone (760 m). The thickness estimates using this stratification approach varied insignificantly in the later works [8, 16–19].

Korneev and Semenov [20–22] first used semiquantitative spectral data for stratification of the Layered Series. Their scheme was based on the rock classification obtained from factor analysis of major and trace element data. These authors proposed somewhat differing schemes for the Aganozero and Shalozero–Burakovo segments (generalized from bottom to top): *ultramafic* zone, *pyroxenite 1* zone, *gabbronorite 1* zone, *pyroxenite 2* zone, *gabbronorite 2* zone, *gabbronorite 3* zone, *pigeonite gabbronorite* zone, *ferrogabbronorite zone*. This scheme is similar to that of Lavrov, with the pyroxenite 1 and gabbronorite 1 zones corresponding to the first megarhythm of the transitional zone, and the pyroxenite 2 and gabbronorite 2 zones, to its second megarhythm.

The first two of the schemes considered were based on the assumption that the magma replenishment did not play a significant role in the evolution of the magmatic system within the chamber. To the first approximation, this allowed one to suggest a single-phase emplacement of the intrusion. New isotopic and geochemical data on the behavior of trace and rare-earth elements in the massif gave rise to concepts of heterogeneity of the Burakovo magma [23], multiple magma intrusion [17, 18], and affiliation of the Aganozero and Burakovo–Shalozero segments to different intrusions [20–22, 24]. Thus, petrological investigations presently tend to complicate the models that explain the origin of the massif. The arguments in favor of multiple intrusion can be divided into several groups: structural, petrographic, geochemical, isotopic–geochemical, and geochronological. Let us briefly consider the main ones.

Petrographic arguments are based on the fact that the Aganozero block is significantly richer in high-Ca pyroxene relative to low-Ca pyroxene as compared to the Shalozero block [22, 24]. It should be noted that physicochemical conditions (pressure, temperature, proportions of liquid and solid phases) inevitably differ in various parts of the chamber of such a large pluton as the Burakovo–Aganozero Massif. This could affect the rock formation at the magmatic and subsolidus stages. We believe that without detailed analysis of phase diagrams the difference in high-Ca pyroxene content cannot definitely indicate the existence of two independent intrusions representing the crystallization products of different magmas.

The Fe number (f') [22] and total REE contents were used to establish the *geochemical differences* between blocks [24]. However, total contents of incompatible elements mainly depend on porosity of the cumulus framework. We suggest that direct comparison of chemical composition of the cumulates without allowance for composition of trapped (equilibrium) liquid is not correct. The attempts of Snyder *et al.* [17] to estimate the REE characteristics of the melt led to geologically contradictory results, since intercumulus melt was not involved in the REE balance during calculations. As a result, they concluded that rocks representing two magmas with different REE characteristics alternate in the massif sections.

Neodymium isotopic data [22–24] are typically used as the strongest argument in favor of multiple intrusion. Amelin and Semenov [23] established that $\varepsilon Nd_{(T)}$ variation exceeds one in the rocks of the Aganozero block. According to the correlation scheme used by these authors, the boreholes sampled for study of Nd isotopic composition characterize different intervals built over each other in the generalized section of the massif. Therefore, such a significant difference in isotopic compositions were accounted for by the formation of the Aganozero block as a result of several intrusions of isotopically different magmas.

According to our concepts reported below, these boreholes are parallel in the section of the pluton and, thus, the scatter in εNd values reflects lateral isotopic variability for the rocks with similar geochemical characteristics. In this case, instead of vertical heterogeneity, we deal with the lateral isotopic zonation closely related to petrogenetic processes within the magma chamber. Thus, based on isotopic data only the conclusion about multiple magma intrusion during the massif formation seems to be premature.

Geochronological arguments [24] are based on Sm–Nd dating of the rocks of the Aganozero and Shalozero blocks yielding a difference of 61 m.y. It is necessary to note that the uncertainty interval caused only by analytical error [25–28] for the accepted estimate of the ^{147}Sm decay constant [29] for the events occurred at 2500 Ma ago is no less than 100 Ma. Therefore, this argument also cannot serve as proof.

In order to create an internally consistent petrological model, it is necessary to determine the structure of the massif and estimate the composition and crystallization conditions of the parental magma, as well as the contribution of subsolidus processes. Such investigations are mainly based on the interpretation of the structure of its Layered Series. The present paper is devoted to this problem.

MATERIAL AND INVESTIGATION TECHNIQUES

About 300 boreholes from 100 to 400 m deep were drilled by PGO Sevzapgeologiya in order to study the massif. Since location of the boreholes was mainly controlled by prospecting goals, our investigation was based on the core from the 160 most representative and petrologically informative boreholes. The work summarizes petrographic study of several hundred thin sections; about 2400 major-element analyses; and more than 10000 semiquantitative analyses for Ti, Cr, Ga, Ni,

V, Co, and Sc,[1] which were kindly provided by the Karelian Geological Expedition.

The accuracy of spectral analysis was controlled for some elements. For this purpose, the results for Ni, Co, and Cr were compared with high-precision determinations performed by N.F. Pchelintseva (personal communication). The calculation results shown in Fig. 2 demonstrates that, in spite of certain systematic deviations, the random component of errors in 70–80% of cases is less than 40 rel. %, which is only two times higher than the typical error of high-precision analyses.

The interpretation of natural material is complicated by the fact that samples for different analyses were taken independently, mainly, from different intervals. Unlike petrographic observations, neither petrochemical nor geochemical data can be directly interpreted. However, the amount of chemical information is several orders of magnitude larger than that of thin sections, and the chemical data are easier to formalize, illustrate, and generalize. Thus, the problem of interpreting petrogeochemical data on the basis of the phase composition of cumulates arose at the initial stage of our study.

The following procedure was proposed to solve this problem. Based on petrographic study, we distinguished the main types of cumulus assemblages in the rocks. Using a set of major-element analyses of petrographically characterized samples, we developed a petrochemical classification, which was most consistent with applied genetic petrographic systematics of cumulus assemblages. All other samples were related to the petrographically characterized ones. Using this procedure we managed to stratify the core petrochemical characteristics and distinguish the intervals with predominant cumulus assemblages, analyze the trace-element distribution on the basis of the most representative rock section, and correlate the borehole sections and construct profiles.

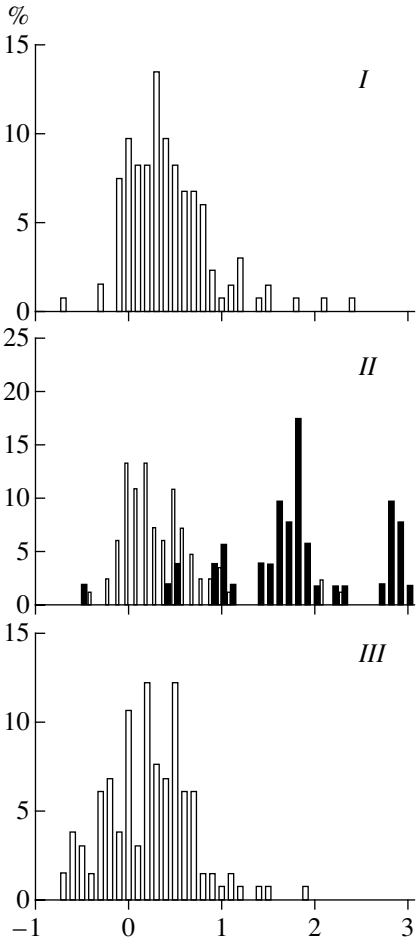

Fig. 2. Correctness of used semiquantitative spectral analyses. (*I*) Ni determinations (n = 133 analyses); (*II*) Co determinations, open boxes are samples with contents <70 ppm (n = 82), filled boxes are samples with >70 ppm (n = 51); (*III*) Cr determinations (n = 131).

RESULTS

Rock Description

Following the petrographic tradition for layered intrusions [30], two textural groups of minerals are distinguished in the rocks of the massif: (1) euhedral to subhedral grains interpreted as cumulus crystals; (2) anhedral grains, rims, and oikocrysts considered as products of intercumulus melt crystallization. The following mineral assemblages were differentiated among the minerals of the first structural group: *Ol, Chr–Ol, Chr–Ol–Cpx, Opx–Cpx, Opx, Cpx, Opx–Pl, Cpx–Pl, Cpx–Opx–Pl, Cpx–Pg–Pl, Mt–Pg–Cpx–Pl*[2] [13, 14, 22]. A more detailed petrographic study additionally recognized rarer cumulus assemblages, for example, *Pl–Pg–Opx* and *Pg–Pl* [31]. The cumulus assemblages distinguished differ in abundance. Most rocks are ascribed only to four of them: olivine, two-pyroxene, two-pyroxene–plagioclase, and two-pyroxene–plagioclase–magnetite. All the other assemblages presumably originated through settling and sorting of crystals during cumulus formation and are subordinate. One of the four major typomorphic mineral assemblages is universally present in each thin section, although some of the minerals are represented only by rare grains.

The proportions of cumulus phases and the cumulus/intercumulus ratio range widely within the massif. Because of this, we consider that it is not reasonable to

[1] The detection limits (in ppm) are as follows: Ti 100, Cr 6, Ga 2, Ni 2, V 4, Co 0.9, Sc 3. Analyses were performed by the electric-arc combustion technique in the Central Laboratory of Northwestern Geological Survey.

[2] Hereafter, the mineral abbreviations are as follows: (*Ol*) olivine, (*Chr*) chromite, (*Opx*) orthopyroxene, (*Px*) pyroxene, (*Cpx*) clinopyroxene, normally augite, (*Pg*) inverted pigeonite, (*Pl*) plagioclase, and (*Mt*) titanomagnetite.

correlate the cumulus and traditional petrographic classifications [30]. Since the names of individual rocks correspond to petrographic tradition, the same petrographic taxon may occur in different cumulus subdivisions.

Olivine cumulates. This group contains dunites, harzburgites, lherzolites, wehrlites, as well as their chromite-bearing varieties. These are greenish gray fine- to medium-grained panidiomorphic or poikilitic massive rocks. *Ol* (60–98%) is euhedral to subhedral 1–3 mm across and intensely serpentinized and occasionally altered to iddingsite. *Opx* and *Cpx* (up to 40%) are anhedral and often altered to bastite. In peridotites, they are represented by equant oikocrysts up to 50 mm in size. *Pl* (up to 10%) fills fine interstices occasionally linked to arachnoidal oikocrysts and is often replaced by bright green serpentine–chlorite or brown saussurite. *Chr* from 0.05 to 3 mm in size is represented either by rare anhedral grains or by octahedral crystals accounting for a few percent of the rock volume. In the latter case, *Chr* is occasionally included in the olivine rims. Biotite (up to 2%) usually develops in small interstices and more rarely forms oikocrysts up to 1.5 mm in size. Trace pentlandite and pyrrhotite are randomly distributed.

Dunites of the Aganozero block normally are ad- or mesocumulates, while orthocumulates are locally developed only in poikilitic peridotites. The interstices are mainly filled by *Cpx* and *Chr* and, more rarely, by *Pl.* Rocks recovered within the Shalozero block are orthocumulates with interstices filled by *Opx, Cpx, Pl*, and *Chr.* With respect to the other silicates, *Cpx* occurs in a subordinate amount. All rocks of the Shalozero block universally contain biotite.

Two-pyroxene cumulates strongly vary in structure and texture and occur in many varieties. This group includes wehrlites, websterites, clino- and orthopyroxenites, melanocratic gabbronorites, and their olivine-bearing varieties, which should be interpreted as transitional from the olivine to two-pyroxene cumulates. These are normally greenish gray, fine-, medium-, or coarse-grained, panidiomorphic and, more rarely, hypidiomorphic rocks (with fragments of resortion and pseudomorphic textures) and have massive or linear structure. *Ol* (up to 40%) is 0.5–3 mm across. In most cases, it is rounded and strongly altered to serpentine with rare relicts of primary mineral.

The euhedral to subhedral *Cpx* (up to 90%) from 0.3 to 3.5 mm across contains exsolution lamellae and occasionally forms simple twins. The low-Ca exsolution lamellae often contain pure chromite crystals no more than a few hundredths of a millimeter in size, which are oriented parallel to crystallographic directions. The mineral is insignificantly altered to light green actinolite hornblende. *Opx* (up to 75%) forms euhedral to subhedral crystals from 0.5 to 3.5 mm in size and occasionally contains droplike inclusions of high-Ca exsolution lamellae. Occasionally, the rocks contain harrisite-like inverted *Pg* (up to 10%) with a characteristic "spruce" exsolution texture, where interstices between lamellae are saturated in vermicular randomly oriented ingrowths of high-Ca pyroxene. The *Pg* intergrowths often extinguish as a single crystal, where high-Ca pyroxene lamellae have similar or various orientations. Microfissures in *Opx* are filled with dirty green chlorite. Anhedral *Pl* (up to 40%) fills interstices or forms tabular oikocrysts up to 10 mm in size, occasionally it is altered to saussurite. Interstices may contain biotite and amphibole. Accessory minerals are Cr-spinel, apatite, zircon, and magnetite. Euhedral *Chr* 0.1 to 0.3 mm in size is enclosed in the interstitial orthopyroxene and plagioclase and locally occurs as inclusions in the olivine and clinopyroxene rims. Of special interest are the nearly monomineral granoblastic and often coarse-grained clinopyroxenites with characteristic mutual serrate simplectitic intergrowths [32]. These rocks contain abundant rounded or dumbbell-shaped enclaves from a few fractions of a millimeter to 15 mm in size, which are filled with quartz, carbonate, feldspars, talc, and amphibole [22]. Such enclaves occur both as inclusions in minerals and in interstices.

The Aganozero block mainly consists of plagioclase-free rocks with *Cpx* significantly predominating over *Opx*. In contrast, the Shalozero block typically contains Pl-bearing rocks that are significantly richer in *Opx.* In addition, they are characterized by universal occurrence of intercumulus quartz, K-feldspar, and biotite (3%). The rocks of this portion of the massif often contain accessory zircon and apatite, which were not found in the Aganozero block.

Two-pyroxene–plagioclase cumulates are represented by gabbronorites, norites, and gabbros. These are light gray (with greenish to brownish tint) leuco- or more rarely mesocratic, fine- to medium- and occasionally coarse-grained or inequigranular rocks with gabbroic or gabbrophitic (with elements of poikilitic or pseudomorphic) textures. The rocks typically have a massive or slightly trachytoid structure; strongly trachytoid varieties are rare. Subhedral (occasionally euhedral) *Pl* (30–90%) 0.6–5.0 mm and up to 7.0 mm long has subparallel orientation and locally forms chadacrysts. It is often cut by fissures that are filled with chlorite. Sometimes plagioclase is strongly altered to saussurite, sericite, carbonate, or epidote. Small plagioclase prisms are enclosed in orthopyroxene or, more rarely, in clinopyroxene, while equant ortho- and clinopyroxene up to 0.3 mm in size are contained in the rims of individual large plagioclase grains. *Pl* hosts acicular magnetite parallel to crystallographic directions [33]. Subhedral *Opx* (up to 40%) 0.7–3.5 mm in size is strongly altered to talc or serpentine and occasionally contains randomly oriented droplike or vermicular ingrowths of high-Ca exsolution lamellae. The upper portions of the Layered Series are dominated by "spurce" inverted *Pg.* As in two-pyroxene cumulates, *Pg* often forms intergowths that extinguish like monocrystal. *Cpx* (up to 40%) is typically hypidiomorphic, 0.3–2.5 mm in size. Occasionally, it forms corroded chadacrysts about 0.4 mm in size in orthopyroxene and

is often intensely altered to green hornblende. The rocks of the upper portion of the section typically contain pyroxenes with variable proportions of solvus phases grading from high-Ca pyroxene matrix with rare low-Ca exsolution lamellae to low-Ca pyroxene matrix with rare high-Ca exsolution lamellae. Quartz (up to 4%) forms fine anhedral crystals. Biotite (up to 2%) 1.0 mm in size is unevenly distributed and associates in interstices with anhedral titanomagnetite 0.3–1.5 mm in size. Accessory minerals are garnet, Cr-spinel, zircon, rutile, apatite, fluorite, chalcopyrite, pentlandite, pyrite, and pyrrhotite.

The rocks of the Aganozero block are abundant in deformed plagioclase crystals. Unlike the Aganozero block, the Shalozero Block is high in interstitial quartz, biotite, magnetite, and apatite and zircon.

Two-pyroxene–plagioclase–magnetite cumulates occur as gabbrodiorites and gabbronorites. These are dark gray, trachytoid, fine-, medium-, or coarse-grained, gabbroophitic rocks with elements of pseudomorphic texture. *Pl* (40–75%) forms subhedral or locally euhedral grains 0.5–3 mm (up to 7 mm) long. *Pl* is rich in small acicular magnetite crystals, as well as albite, chlorite, epidote–zoisite, and sulfides, which develop along fissures. Subhedral *Cpx* (10–30%) 0.8–4.5 mm in size is occasionally altered to green hornblende and biotite. Equant *Pg* (10–20%) grains 0.5–2.5 mm in size often form intergowths. Occasionally, *Pg* is replaced by tremolite–actinolite. Like the rocks representing the two-pyroxene-plagioclase cumulates, these rocks often contain pyroxene with variable proportions of solvus phases. Subhedral titanomagnetite (3–15%) 0.3–1.7 mm in size often includes fine exsolution lamellae of ilmenite and rims of biotite. Quartz, biotite, and K-feldspar account for about 3% with sporadic occurrence of anhedral quartz (<1%) up to 0.7 mm in size. Accessory minerals are apatite, chalcopyrite, and pyrrhotite.

Thus, the petrographic data indicate long-term thermal evolution of the massif completed by widely developed subsolidus processes, namely, deformation and recrystallization of cumulus minerals, breakdown of pyroxene solid solutions, and crystallization of the Cr- and Fe-bearing phases respectively in clinopyroxene and plagioclase. Petrographic study also demonstrates systematic differences between the rocks in different blocks. The Aganozero block consists of adcumulates, whereas the Shalozero block mainly contains orthocumulates with wide development of the low-temperature intercumulus minerals: plagioclase in olivine and two-pyroxene cumulates, quartz, biotite, apatite, zircon, magnetite, and K-feldspar. These observations make it possible to assume a higher residual porosity (after [34]) of the cumulus framework in the Shalozero rocks than in the Aganozero rocks.

Major-Element Chemistry

In order to interpret the major-element variations observed, it is necessary to develop a method for dividing the available data into groups corresponding to the main cumulus assemblages distinguished during petrographic study. A numerical procedure for cumulus sytematics was proposed, which takes into account specific features of the rocks. The reference sampling involved only the analyses of the petrographically described rocks. The rocks were subdivided into groups according to their cumulus assemblages. Each chemical analysis consisting of n element determinations was represented as an n-dimensional vector normalized to its length. Thus, the compositional sampling may be represented by data points on the surface of an n-dimensional hypersphere of a unit diameter. Some ε area can be given for each point on the hypersphere surface. Two compositions, reference and tested, can be considered to be identical if the distance ρ between them is less than ε. If too small an ε value is chosen, some tested analyses may have no counterparts in the reference sampling. On the other hand, too large an ε value may lead to an erroneous classification. If the analyses in the reference sampling are evenly distributed over the entire compositional range, it is reasonable to set an ε value that would provide reliable identification of compositions in 85–90% of cases. It was empirically found that this value should be twice as high as the error of silicate analysis. Using this procedure, we classified the whole body of petrochemical data.[3] Data on different blocks were processed separately.

The bulk Fe number f' calculated as the Fe/(Fe + Mg) atomic ratio can be taken as an index reflecting the evolution of the intrusion. In most cases, this parameter monotonously changes in the course of magmatic evolution and weakly depends on the proportions of Fe–Mg minerals and feldspars. This index increases with accumulation of iron oxides in the rock. The irregular distribution of magnetite in the Layered Series rocks may lead to a significant variation of the bulk Fe number throughout the section. In this case, the lower curve enveloping these variations should be considered as the locus of efficient f' values including the rock evolution.

As an example, Fig. 3 demonstrates the variations of SiO_2 and FeO contents relative to f' in the rocks of the intrusion. It is seen that f' gradually increases in the rocks corresponding to the main cumulate types from

[3] In this paper, the following angular distance was used as the distance between compositions X and Y: $\rho_{(X, Y)} = \sqrt{\sin^2\Theta}$, where $\Theta = \arccos\frac{\sum_{i=1}^{n} X_i Y_i}{\sqrt{\sum_{i=1}^{n} X_i^2 \sum_{i=1}^{n} Y_i^2}}$, while X_i and Y_i are molecular amounts of i-component in compositions X and Y.

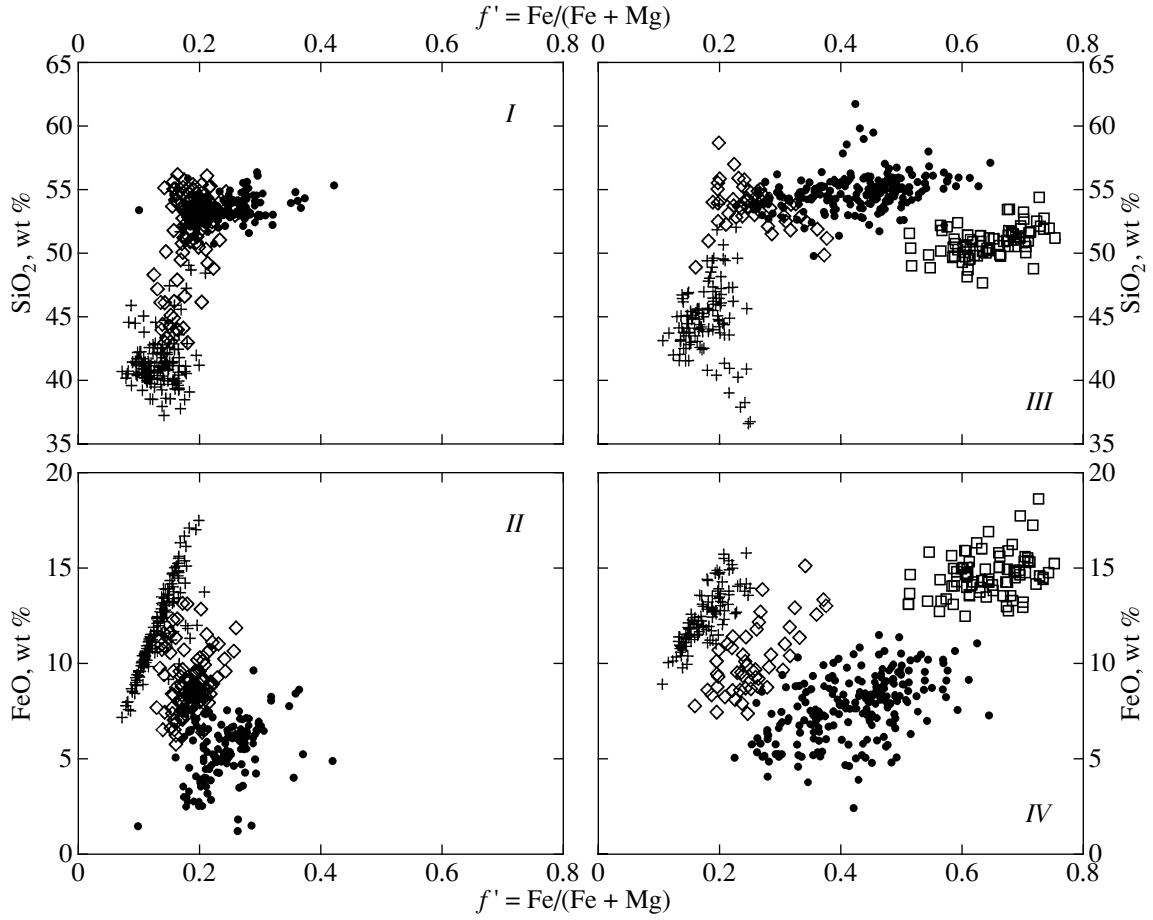

Fig. 3. Major-element variations versus bulk Fe number f' in the rocks of the Aganozero (*I–II*) and Burakovo–Shalozero (*III–IV*) segments of the massif. Symbols: crosses are olivine cumulates, diamonds are two-pyroxene cumulates, circles are two-pyroxene–plagioclase cumulates, and boxes are two-pyroxene–plagioclase–magnetite cumulates.

olivine through two-pyroxene and two-pyroxene–plagioclase to two-pyroxene–plagioclase-magnetite assemblages. The data points of rocks with certain cumulus assemblages form sublinear clusters along the liquid lines of descent controlled by corresponding liquidus assemblages. This supports the correctness of the performed discrimination.

The bulk Fe number of a rock is related to the composition and proportions of the constituent phases. The amount of trapped intercumulus melt affects this index significantly more than the proportions of silicate minerals in the cumulus framework, since the Fe/Mg ratios in the coexisting olivine and pyroxenes differ insignificantly but are always significantly lower than those in the equilibrium melt.

This feature of f' behavior should be taken into account during interpretation of petrochemical data in the individual blocks of the massif. Unlike the Aganozero block, the rocks of the Shalozero–Burakovo part of the massif has a systematically higher Fe number: 0.18 ± 0.03 against 0.13 ± 0.03 for olivine cumulates, 0.25 ± 0.05 against 0.18 ± 0.03 for two-pyroxene cumulates, and 0.35 ± 0.07 against 0.24 ± 0.04 for pigeonite-free two pyroxene-plagioclase cumulates. In addition, the Shalozero-Burakov rocks are systematically higher in Ti content. Histograms for the rocks with incompatible Ti are presented in Fig. 4.

Thus, the facts of the systematic differences in bulk Fe number and Ti content between the rocks from different parts of the massif are consistent with the assumption of different porosities of cumulus frameworks (proportions of "trapped" melt), which is based on petrographic data. Different porosities can also be expected from data on the relief of the plutonic chamber floor (Fig. 1): the denser cumulate should be confined to the central part of the funnel-shaped Aganozero Block; the "looser" cumulus framework, to the peripheral parts of the Shalozero block, which has a low-angle floor. This conclusion contradicts the suggestion that the differences in major- and trace-element compositions of rocks in the Aganozero and Burakovo-Shalozero segments of the massif are related to the diversity of the primary magmas for these blocks. It is evident that, because of the different proportions of cumulus and intercumulus phases, the "synchronous" rocks, i.e., the rocks crystallized from the same magma in different

blocks, can be misinterpreted as products of different stages of the magma evolution or even as products of different magmas.

Trace-Element Geochemistry

The aim of the proposed geochemical analysis is to develop a method for interpreting spectral determinations of individual samples. This approach is based on the regular distribution of trace elements in rocks, which can be approximately described using mineral–melt partition coefficients. The distribution of some compatible elements, such as Ni, Co, Cr, Ti, V, Sc, and Ga, whose accumulation mainly depends on the proportions of cumulus minerals, is (very) extremely important for subsequent analysis of the stratigraphy of the Layered Series.

In spite of significant differences in the partition coefficients of these elements for rock-forming minerals, it is difficult to interpret genetically the data on the distribution of these elements along the borehole sections because of significant variations of their concentrations. Therefore, the ratios of elements rather than their absolute values were used in our consideration. The examination of element ratios has some advantages. First of all, the diagram has greater contrast owing to the higher sensitivity of element ratios to the proportions of minerals concentrating these elements. At the same time, the ratios are less sensitive to variations caused by the presence of additional mineral phases with subordinate amounts of these elements. Trace-element abundances in the rocks may differ by several orders of magnitude. For convenience, the element concentrations were divided by 10^3 for Ti, Mn, Cr, and Ni; by 10^2 for V, Co, Sr; and by 10^1 for Ga and Sc.

The ratio of elements concentrated mainly in different minerals reflects the proportions of these minerals in the rock. According to their partition coefficients, V and Sc are mainly accumulated in high-Ca *Px*, while Ga is mainly distributed in *Pl*. Thus, the V/(Ga + V) and Sc/(Ga + Sc) ratios reflect the proportions of high-Ca *Px* and *Pl*. The highest values of these ratios are typical of pyroxenites, while the lowest values, to gabbroids. However, because of the high partition coefficient of V for Cr-spinel or titanomagnetite, the V/(Ga + V) ratio cannot be uniquely interpreted for rocks with significant proportions of these minerals. Nickel is mainly concentrated in *Ol*. Therefore, the Ni/(V + Ni) ratio should reflect the proportions of *Ol* and high-Ca *Px*. The highest Ni/(V + Ni) ratios typically occur in the *Ol*-rich rocks, while the lowest ones occur in the olivine-free cumulates. The variations of this ratio in the rocks composed of the olivine cumulates may be related to the presence of intercumulus high-Ca *Px* or chromite.

The ratios of elements concentrated together in one or several coexisting minerals are defined by several factors: the extent of evolution of the melt that generated the cumulus mineral assemblage, the cumulus–intercumulus ratio, and the modal composition of the rocks. Thus, the vertical variations of these ratios may be used together with petrochemical indices *f*' and *an*' for correlating rock sections [13, 14]. In our case, the most informative ratio is Co/(Co + Ni) [35], which is sensitive not only to certain differences in behavior of these elements during crystallization of olivine concentrating these elements, but also to the character of melt evolution at final stages. It should be taken into account that sulfide mineralization in the rocks increases the bulk content of Ni more rapidly than that of Co, thus resulting in strong variations of the corresponding ratio.

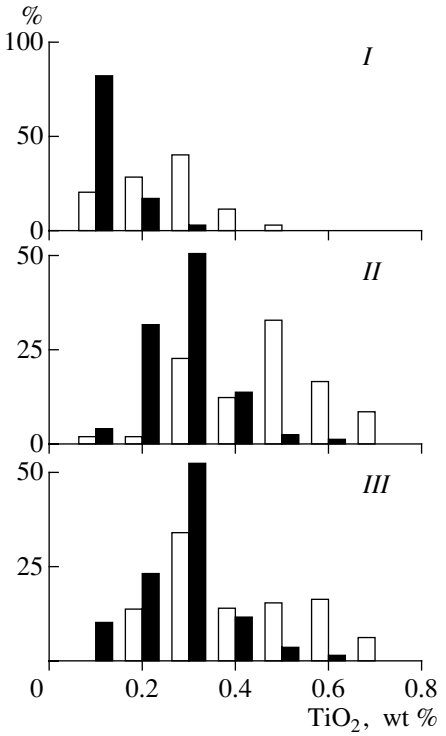

Fig. 4. Histogram of Ti contents in the rocks of the Aganozero (dark) and Burakovo–Shalozero (light) segments of the massif. (*I*) Olivine cumulates (628 and 114 analyses for the Aganozero and Burakovo–Shalozero parts, respectively), (*II*) two-pyroxene cumulates (339 and 50 analyses), and (*III*) two-pyroxene–plagioclase cumulates without inverted pigeonite (288 and 87 analyses).

The efficiency of the proposed approach may be demonstrated for boreholes 200 and 331, because all types of cumulus assemblages can be observed there (Fig. 5). Borehole 200 penetrated two-pyroxene–plagioclase, pyroxene, and olivine cumulates of the Aganozero block and reflects the element distribution at the early stages of magma evolution. Borehole 331 drilled into the Shalozero–Burakovo block penetrated the transition zone from two-pyroxene–plagioclase to magnetite–two-pyroxene–plagioclase cumulates and reflects the element distribution at the late stages of magma evolution. Together with trace-element variations, Fig. 5 demonstrates the results of identification of cumulus assemblages by major-element contents in the rocks.

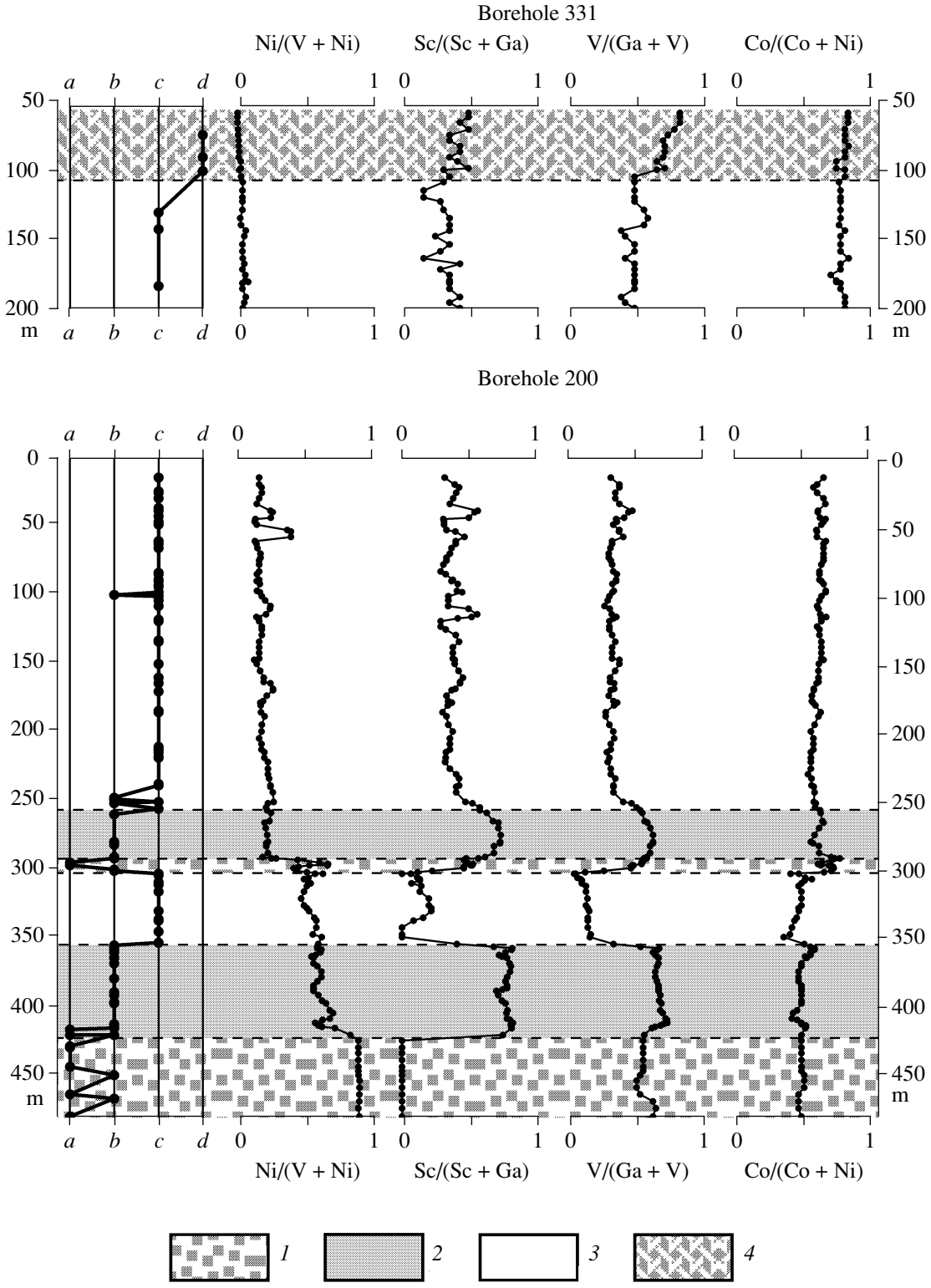

Fig. 5. Petrochemical systematic of cumulates and variations of trace-element ratio in the rocks of boreholes 200 and 331. Results of petrochemical systematics: (*a*) olivine cumulates, (*b*) two-pyroxene cumulates, (*c*) two-pyroxene–plagioclase cumulates, (*d*) two-pyroxene–plagioclase–magnetite cumulates. Zones with predominant development of (*1*) olivine cumulates, (*2*) two-pyroxene cumulates, (*3*) two-pyroxene–plagioclase cumulates, (*4*) two-pyroxene–plagioclase–magnetite cumulates.

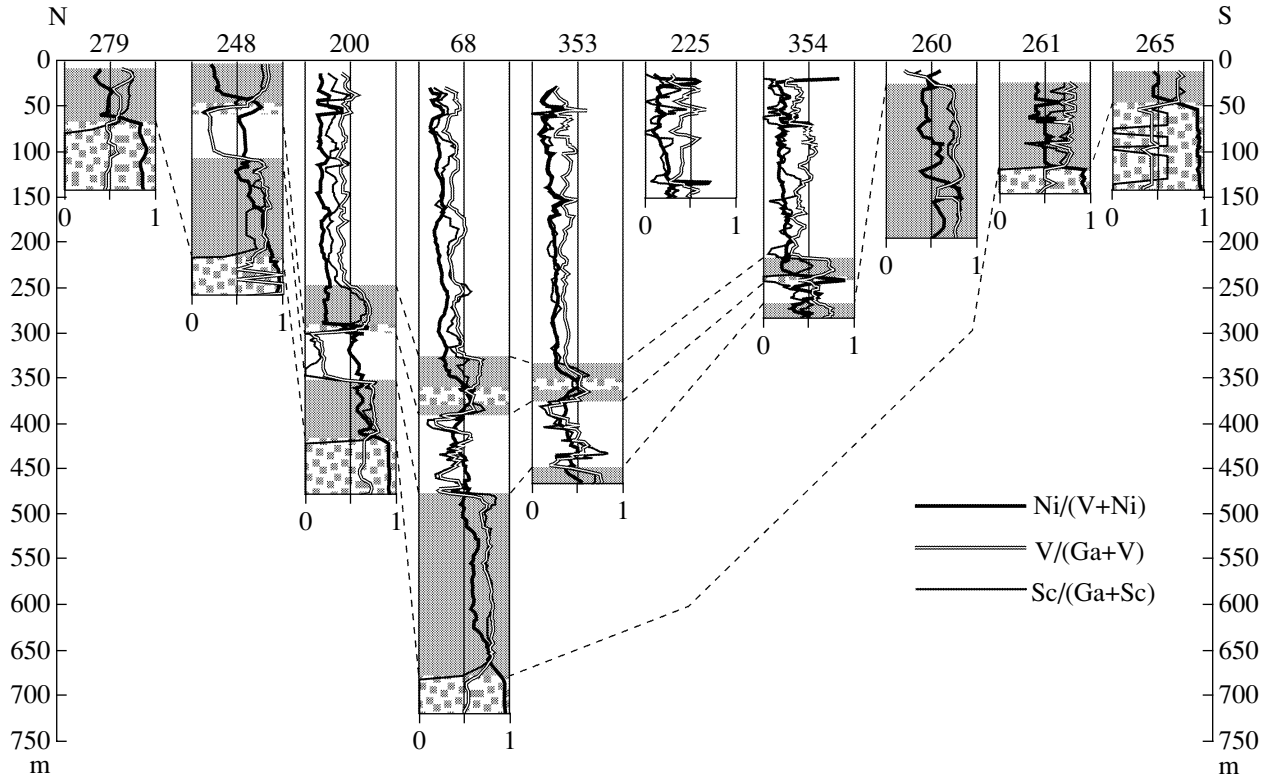

Fig. 6. Geochemical structure of the Aganozero block, N–S trending profile. See Fig. 5 for symbol explanation.

The petrochemical and geochemical data show a good correlation, but the geochemical indices seem to be significantly more informative owing to denser sampling.

Correlation of Rock Sections; Reconstruction and Examination of Profiles across the Burakovo–Aganozero Intrusion

The geochemical principles stated above make it possible to correlate rock sections, reconstruct the geochemical structure of different blocks of the intrusion, and propose a generalized section of the massif.

Geochemical structure of the Aganozero block. The Aganozero block is almost completely composed of the olivine cumulates at the present erosion level. All other differentiates account for slightly more than 1 vol % and are located in its central part, forming a N–S-trending synclinelike structure. This syncline composes a closed structure, which is well expressed in the profiles. Many boreholes that intersect the syncline rocks were terminated in the underlying peridotites, thus facilitating the correlation of section of the Layered Series.

The structure of the block is well illustrated by a N–S-trending profile (Fig. 6). Unlike the traditional lithologic profiles reflecting the distribution of rock varieties, the geochemical profile shows the distribution of chemical elements in the rocks. In Fig. 6, the geochemical structure of the massif is characterized by variations of three elements ratios. Such a geochemical structure corresponds to the following cumulate sequence: olivine, two-pyroxene, and two-pyroxene–plagioclase. A distinctly expressed structure of the two-pyroxene cumulates is observed throughout the entire profile as two V/(Ga + V) or Sc/(Ga + Sc) maxima separated by their minimum. The lower part of the upper maximum coincides with a local Ni/(V + Ni) maximum. This indicates that the two-pyroxene cumulates are complicated by the layers of peridotites and leucocratic gabbronorite to anorthosites. The two-pyroxene–plagioclase cumulates show low and variable V/(Ga + V) and Sc/(Ga + Sc) ratios and are complicated by scarce Ni/(V + Ni) maxima. Such a structure may be interpreted as an alternation of gabbroids with a variable mafic index, which contain olivine-rich horizons.

It is most distinctly expressed in the northern part of the syncline (boreholes 248 and 200). In its southern part (borehole 68), the section changes, retaining only general characteristics. In particular, upsection, beginning from the gabbronorite–anorthosite unit of the two-pyroxene zone, the geochemical structure becomes less contrasting and we can only talk about the predominance of a certain rock type: more leucocratic gabbroids are complicated by rhythmically layered beds of pyroxenite and melanocratic gabbros, whereas pyroxenites, especially the lower portion of the pyroxenite unit, are complicated by melanocratic gabbros. The location of the peridotite layer somewhat changes. It is restricted to the contact between the units in the mar-

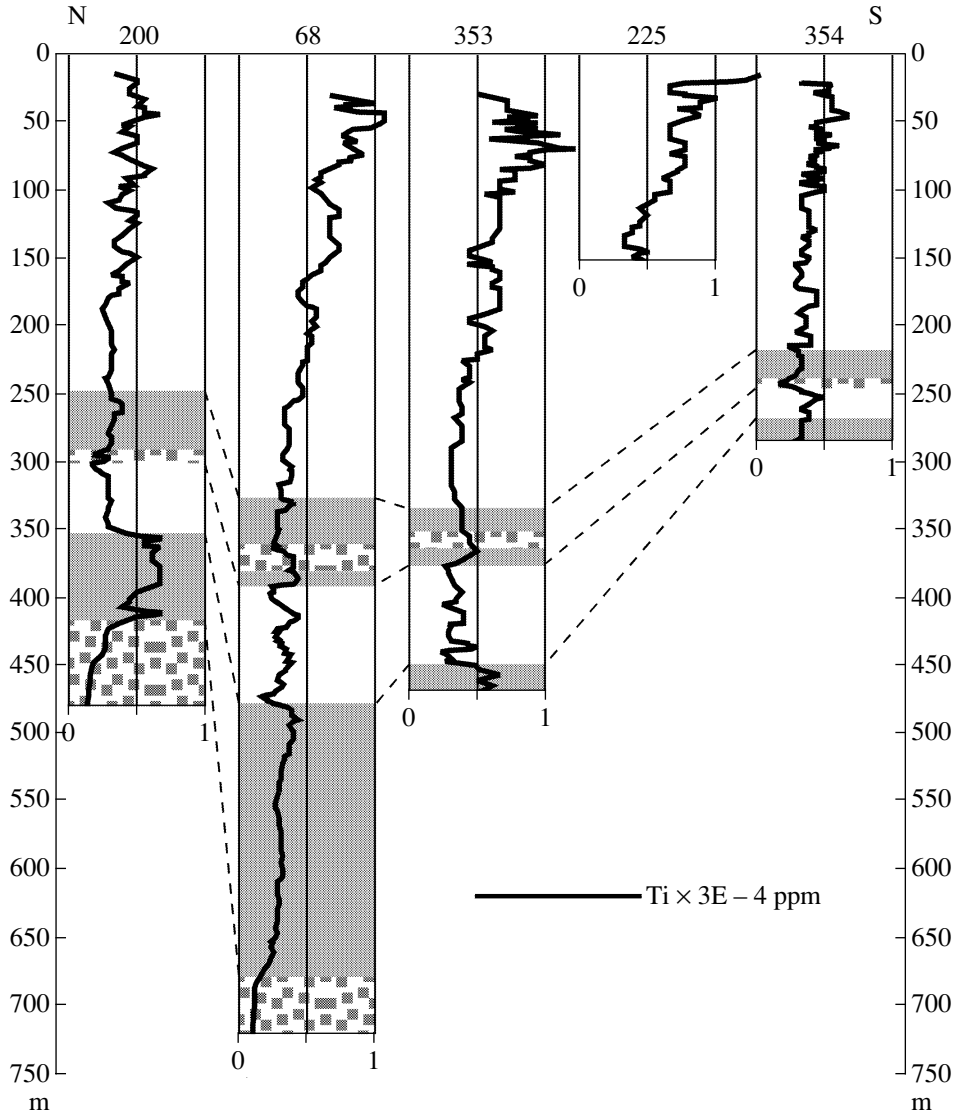

Fig. 7. Variations of Ti content in the rocks of the central part of the Aganozero block. See Fig. 5 for symbol explanation.

ginal parts of the syncline and occurs somewhat higher, in the lower part of the pyroxenite unit, in the central part of the syncline. The absence of reduction of the two-pyroxene cumulate thickness at the southern termination of the syncline, as well as strong differences in the stratigraphic height of sections in boreholes 354 and 260 separated by a distance of 500 m may indicate the existence of a fault cutting off the southern part of the gabbroid body.

The upsection increase in Ti contents in gabbroic rocks allows us to determine the uppermost horizons of the Layered Series of the Aganozero block. Anomalously high Ti contents are observed in the upper portions of boreholes 68, 225, and 353 (Fig. 7).

It is clearly seen that the rock section in borehole 200 differs from those in the adjacent boreholes 248 and 68 in having reduced thicknesses of stratigraphic units. This can be explained by the different position of the boreholes with respect to the thalweg of the ravine-like roof of the ultramafic zone. Boreholes 248 and 68 are located significantly closer to the syncline axis, while borehole 200 is projected upon its western limb. Because of this, we can suggest that the axis of the Aganozero syncline is arcuate in plan. This assumption is well consistent with the structure of the section in borehole 201, which was drilled west of borehole 200 and repeats its structure in detail. The rock units in this section have even more reduced thicknesses, and the layer of leucocratic gabbroids is thinned to about 15 m.

Geochemical structure of the Shalozero–Burakovo part of the massif. Unlike the Aganozero block, the Shalozero–Burakovo part of the massif has been significantly less studied. This is related not only to the lower density of the borehole net, but also to the specific structural features of the block. The gabbroic rock

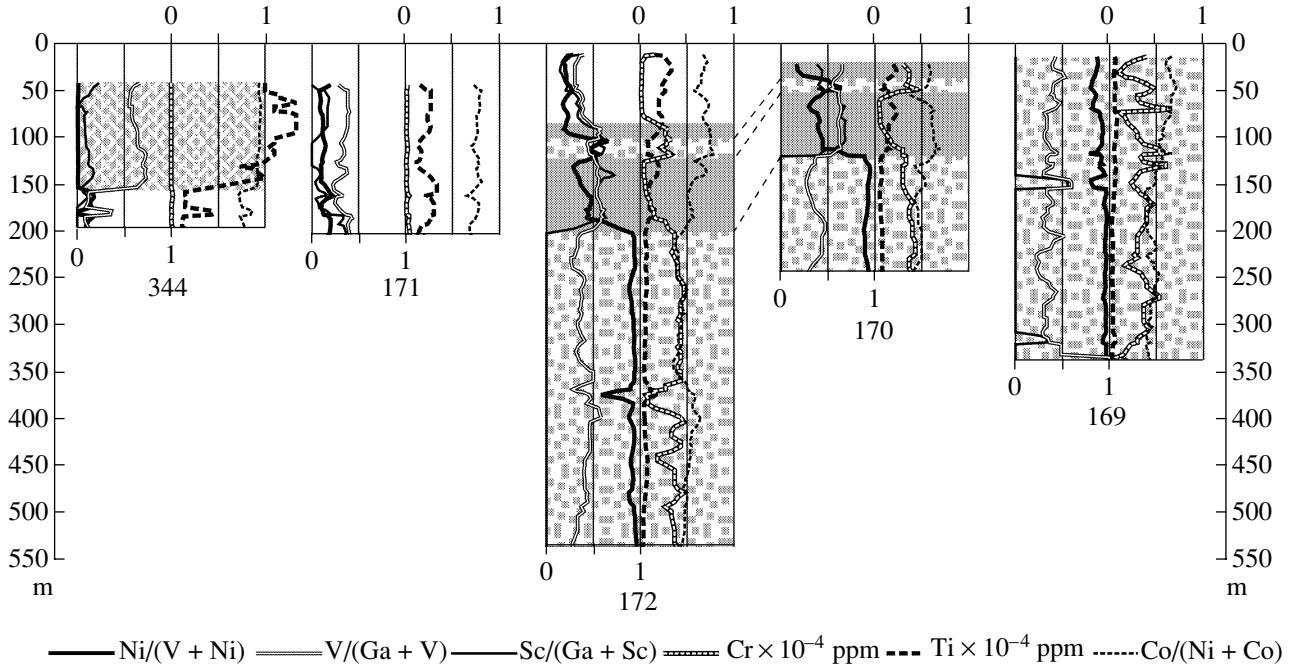

Fig. 8. Geochemical profile across the eastern part of the Shalozero block. See Fig. 5 for symbol explanation.

thicknesses increase sharply inward the Shalozero–Burakovo block because of the lowering of the ultramafic rock roof and the existence of the uneroded higher horizons of the Layered Series. In addition, the Layered Series of the Shalozero–Burakovo segment of the intrusion is petrographically much less variable than the Layered Series of the Aganozero block. All these factors considerably complicate the recognition of synchronous horizons. Some unrecovered deeper horizons of unknown thickness may exist in the Layered Series.

The rock section of two types with different geochemical structures were penetrated within the Shalozero block. Type 1 sections were found only in boreholes 174 and 175 located at the northeastern termination of the block, in the junction zone with Aganozero block. The geochemical structures of these sections are very similar to the structure of the sections in the marginal parts of the Aganozero syncline.

Type 2 sections are typical of the entire block and can be characterized by the profile that intersects cumulates of all types found in the massif (Fig. 8). The unit of the two-pyroxene cumulates (boreholes 170 and 172) has a simpler structure consisting mainly of pyroxene-rich rocks complicated by a peridotite layer. The transition from two-pyroxene–plagioclase to magnetite–two-pyroxene–plagioclase cumulus assemblages is observed in borehole 344 and marked by a sharp increase in the V/(Ga + V) ratio. This assemblage is different in that it has the highest Ti content.

The section of type 2 distinctly differ from those of type 1 in the absence of a gabbroic layer beneath the peridotite horizon. At the same time, the identical geochemical structures of sections in boreholes 174 and 175 and in the gabbroic syncline of the Aganozero block may indicate a closer relation of these sections to the Aganozero block than to the Shalozero blocks. This fact may be explained by the existence of an imbricate thrust fault in the junction zone between the Aganozero and Shalozero blocks.

The geochemical structure of the Layered Series recovered at the western margin of the Shalozero block is characterized by the profile shown in Fig. 9. The profile boreholes intersect two-pyroxene and magnetite–two-pyroxene–plagioclase cumulates. The lower boundary of the unit of the magnetite–two-pyroxene cumulates (borehole 45) is marked by a sharp increase in the V/(Ga + V) ratio and Ti content. The sections that penetrated this cumulus assemblage were correlated on the basis of the Co/(Ni + Co) ratio. Since this ratio varies within the sections, only general variation trends were used in the correlation scheme. The distribution of this ratio is well consistent with the distribution of V/(Ga + V) values. The appearance of *Mt* (V concentrator) in the Layered Series leads to a strong increase in V in the rocks. As *Mt* crystallizes, V is removed from the melt, and its content decreases in the Layered Series at approximately stable Ti contents.

There are insufficient data to construct representative profiles across the *Burakovo block*. Consequently, the rock sections were examined with the aim of searching for an upper border zone, a sandwich horizon, or the most differentiated horizons of the Layered Series. However, none of the boreholes drilled in the Burakovo block has revealed geochemical structures

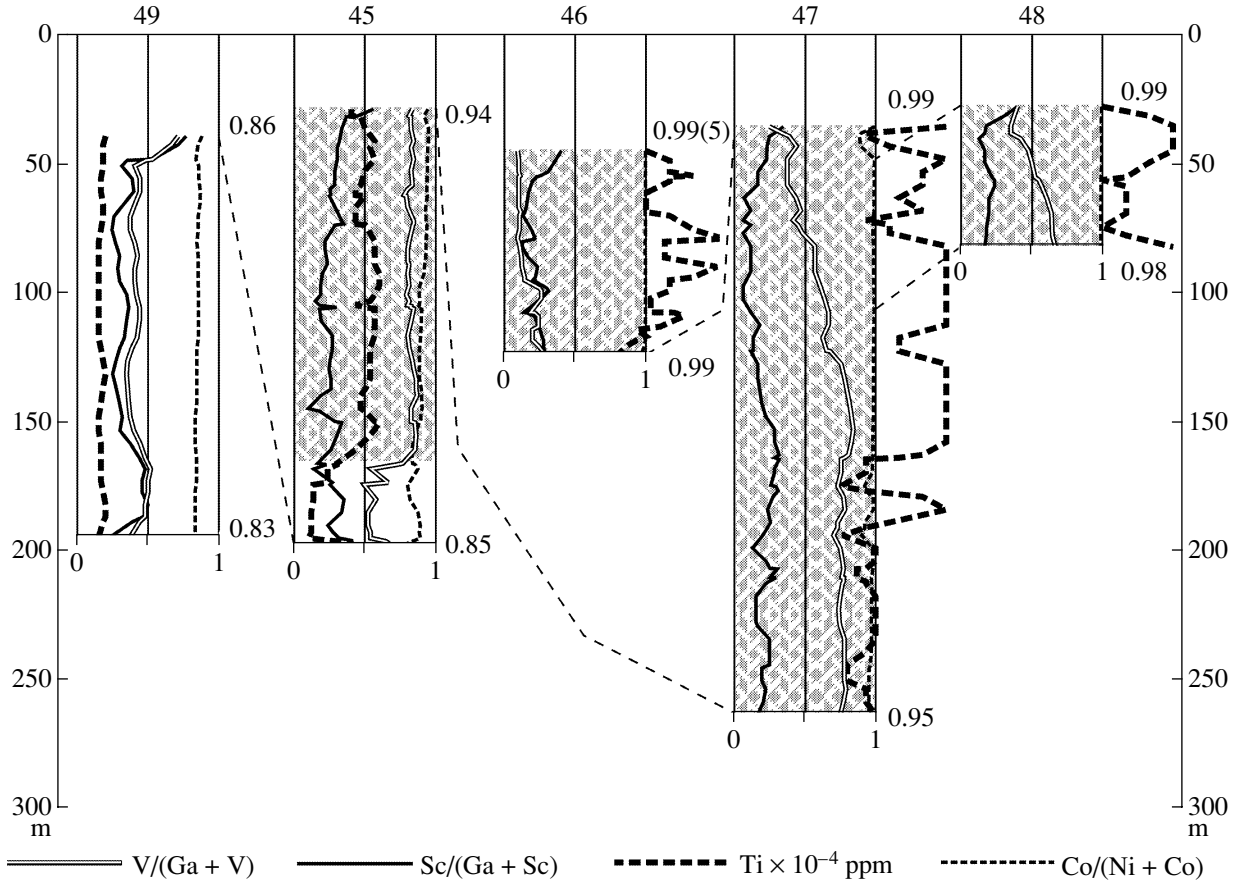

Fig. 9. Geochemical profile across the western part of the Shalozero block. See Fig. 5 for symbol explanation. Numerals at the top and bottom of sections are the maximum values of the Co/(Ni + Co) ratio.

typical of the upper border zone. A complete section of the upper border zone should demonstrate a reverse petrographic zonation, while an incompletely preserved section should show a reverse trend of Co/(Ni + Co) variation. In addition, this ratio in the studied rocks of the Burakovo block is lower than their values in the rocks recovered by borehole 46 in the Shalozero block. These observations suggest that the complete section of the Layered Series has not yet been penetrated, and the most differentiated horizons of the Layered Series were found in borehole 46.

Generalized Section of the Burakovo–Aganozero Intrusion

Our investigations made it possible to compile a generalized section of the Layered Series of the intrusion. According to regular changes of cumulus assemblages in the profile sections above, the Layered Series of the pluton is subdivided into four zones (from bottom to top): olivine cumulates, two-pyroxene cumulates, two-pyroxene–plagioclase cumulates, and magnetite–two-pyroxene–plagioclase cumulates. The volume proportions of rocks cannot be estimated at this stage with the accuracy required for balance calculations. The apparent thicknesses of zones reported below are only approximate.

Zone of olivine cumulates. According to geophysical data, its thickness is estimated to be 3 km within the Shalozero–Burakovo block [3] and 6 km including the upper 900-m portion of completely serpentinized rocks in the Aganozero block [3, 7]. On the basis of the cumulus/intercumulus ratio, this zone is traditionally subdivided into two subzones: dunite and poikilitic peridotite. The dunite subzone is available for direct investigations only within the Aganozero block. It consists of homogeneous olivine adcumulates with insignificant variations of cumulus (95–98%) and intercumulus (2–5%) assemblages.

The poikilitic peridotite subzone is composed of the rocks with a “loose” cumulus framework, where, according to petrographic study, intercumulus accounts for 10–20%, occasionally reaching 40%. The apparent thickness of this subzone ranges from 360 to 600 m. Intercumulus in different blocks differs in composition. In the Aganozero block, the subzone is dominated by poikilitic wehrlites, which include rare 2 to 10-m-thick horizons of lherzolites and harzburgites. Some sections contain pyroxenite and dunite horizons of variable

thicknesses and thin interlayers of chromite ores. This subzone in the Shalozero block mainly consists of poikilitic lherzolites and harzburgites and lacks pyroxenite and chromitite horizons. It is interesting that the section in the junction zone between the Aganozero and Shalozero blocks (boreholes 174–175) is mainly composed of lherzolites with rare harzburgite horizons, whereas the section in the southern part of the Shalozero block is dominated by harzburgites with thin wehrlite interlayers restricted to the upper part of the subzone. This observation once again demonstrates the transitional character of the junction zone with respect to both blocks.

Zone of two-pyroxene cumulates has the most complex structure. The apparent thickness ranges from 100 to 350 m within the Aganozero block and from 60 to 180 m within the Shalozero block.

Within the Aganozero block, this zone is higher in clinopyroxene with respect to orthopyroxene. Two-pyroxene cumulates are typical of the upper portions of this zone, whereas clinopyroxenites are mainly restricted to its lower part. Olivine cumulates are separated from two-pyroxene cumulates by a transitional zone 5–10 m thick, where peridotite cumulates are intensely altered to clinopyroxenite aggregate, thus forming spotty rocks with peridotite relics [16, 22]. It is interesting that clinopyroxenites are mainly confined to the central parts of the Aganozero syncline, while websterites are confined to its periphery [31]. It was also found that basal horizons in the central parts of the zone contain unique nearly monomineral clinopyroxenites with typical granoblastic textures and serrate simplectitic intergrowths. Clinopyroxenites are characterized by the wide development of quartz–carbonate inclusions both in cumulus and in intercumulus minerals [22]. Pyroxenite zone recovered in the Shalozero–Burakovo block mainly consists of websterites. Unlike in the Aganozero block, the pyroxenite zone here is higher in orthopyroxene and its rocks lack evidence of subsolidus alteration.

In both parts of the massif, the zone is complicated by a peridotite layer (olivine–orthopyroxene–chromite cumulates) with apparent thickness from 5–8 m in the Aganozero block (boreholes 68, 248) to 40 m in the southern part of the Shalozero block (boreholes 333, 334). Asymmetric changes in thickness of this layer (which do not concur with the regularities established for the other rocks of the Layered Series), the variable stratigraphic position within the zone, the recurrence of crystallization order, and the accumulation of a thick layer of the more primitive cumulus assemblage may be explained by an additional injection of less fractionated magma. Evidently, the additional injections are occasional events; therefore the nearly identical stratigraphic position of the peridotite layer in the sections of both blocks suggests their coeval formation. This indicates that the pluton is a single geological body.

The zone of two-pyroxene cumulates within the Aganozero block is complicated by the layer of leucogabbroids and anorthosites. It is located below the peridotite horizon. The thickness of the layer varies laterally from 60 m in the northern part of the syncline to 90 m in its central part. In the north of the syncline (boreholes 16 and 200), the layer is represented by gabbronorites with websterite interlayer. In the central part of the syncline (borehole 68), the amount of thin interlayers of websterites, clinopyroxenites, and peridotites increases, and the layer grades into a contrast layered sequence. The section of the layer is completed by an anorthosite horizon several meters thick, which is traced along the entire structure. The central part of the block is characterized not only by the highest thickness of the leucogabbroid layer, but also by the presence of gabbronorite and anorthosite interlayers in the upper part of the pyroxenite zone. These interlayers also thin out to the syncline periphery. Gabbroid rocks in the upper pyroxenite layer account for no more than 5–10% of the total thickness of the section [31].

The absence of the described stratigraphic unit in the available rock sections in the Shalozero–Burakovo segment, the highest thickness of this unit in the central part of the Aganozero block, and its thinning out at the margins of the syncline indicate a limited abundance of these rocks and their relation to horizons of the strongest subsolidus alteration.

Zone of two-pyroxene–plagioclase cumulates mainly consists of gabbronorites and gabbronorites with inverted pigeonite. Anorthosites, gabbros, norites, and plagioclase-bearing websterites occur in subordinate amounts, forming rare horizons and thin layers. Only the lowermost 300-m-thick part of this zone remained uneroded within the Aganozero block. At the Shalozero block, the entire section with this zone of apparent thickness >750 m was recovered in boreholes.

A characteristic feature of this zone is the replacement of orthopyroxene by inverted pigeonite. In the previous schemes of the massif structure [11, 12, 22], the transition to the rocks with inverted pigeonite was used as a stratigraphic boundary. However, its stratigraphic position is variable. In particular, the rocks of the Aganozero block with increased thickness owing to its funnel shape contain pigeonite at a height of 200 m from the lower boundary of the zone. At the same time, the rocks of a 385-m-thick section of this zone in the Shalozero block (borehole 333) are devoid of pigeonite.

Pigeonite gabbronorites of the Aganozero block have apparent thickness of about 60 m. They present an alternation of rapidly thinning out layers and lenses of websterites, orthopyroxenites, norites, anorthosites, gabbronorites, and gabbronorites with inverted pigeonite. The latter rocks are dominant. The layer bears evidence of subsolidus alteration. The rocks show spotty or banded structures; taxitic and pegmatoid varieties are abundant. Compared to the underlying gabbronorites, pigeonite gabbronorites are characterized

by significantly more extensive secondary alteration with the development of scapolite, chlorite, prehnite, carbonate, and talc.

The pigeonite gabbronorite unit of the Shalozero–Burakovo block is layered, with alternation of 20 to 30-m-thick layers of pigeonite gabbronorites and 1 to 4-m-thick horizons of some other rocks (mainly gabbronorites without inverted pigeonite, and, more rarely, anorthosite, websterites, and pigeonite websterites) [31]. Gabbronorite horizons are often complicated by interlayers of norites, anorthosites, ferrogabbronorites, and taxitic rocks. Such complex relations between ordinary gabbroids and their pigeonite counterparts presumably resulted from subsolidus alteration of low-Ca pyroxene to its polymorph on cooling.

Zone of two-pyroxene–plagioclase–magnetite cumulates is mainly composed of titanomagnetite gabbronorites. The layering of the zone is mainly represented by rhythmic alternation of leuco- and mesocratic gabbroids. The layers of melanocratic gabbronorites, websterites, norites, and anorthosites account for an insignificant part of the total volume of the zone, no more than 5–6%. The layers of mesocratic rocks often show a microrhythmic structure caused by regular variations in content of cumulus titanomagnetite. Plagioclase and titanomagnetite contents generally increase upsection, while the pyroxene content proportionally decreases. The apparent thickness of the zone is 450 m.

Thus, the sequence of zones in the Layered Series corresponds to typomorphic cumulus assemblages: *Ol* ⟶ high-Ca *Px* + low-Ca *Px* ⟶ high-Ca *Px* + low-Ca *Px* + *Pl* ⟶ high-Ca *Px* + low-Ca *Px* + *Pl* + *Mt*. In the first approximation, it may be taken as the crystallization sequence of the primary magma of the Burakovo–Aganozero pluton.

DISCUSSION AND CONCLUSIONS

The proposed stratification and correlation schemes are formally similar to those reported in [22]. However, the factors used for classification in the cited paper cannot be correctly interpreted from the geochemical viewpoint. Note that large factor loadings (0.7–0.8) characterize loss on ignition and slightly incompatible Mn, which are difficult to interpret petrologically. The absence of a clear interpretation of the analytical material studied determined many inaccurate conclusions of these authors. For example, the section of the Border Group penetrated by borehole 187 was ascribed to the Layered Series.

The simple and efficient method proposed in our paper has clear geochemical meaning, and each sample can be characterized by a certain phase composition. The proposed algorithm of petrochemical systematics favorably differs from traditional statistical procedures based on calculation of average values. For the correct use of these procedures, the studied sampling should be convex. Otherwise, this procedure may generate average values falling beyond the analyzed sampling.

The following conclusions can be drawn from our investigation.

(1) A simple and efficient method of phase interpretation of petrochemical and geochemical information was proposed, which allows one to use chemical analyses without thin-section observations.

(2) The available petrographic data suggest that all the diversity of accumulative rocks is defined by one of four typomorphic mineral assemblages: *Ol*, high-Ca *Px* + low-Ca *Px*, high-Ca *Px* + low-Ca *Px* + *Pl,* and high-Ca *Px* + low-Ca *Px* + *Pl* + *Mt*.

(3) A new structural scheme of the Layered Series of the Burakovo–Aganozero pluton was proposed. It was shown that the Layered Series of the intrusion has the following succession of cumulate zones: olivine, two-pyroxene, two-pyroxene–plagioclase, and magnetite–two-pyroxene–plagioclase. This succession corresponds to the sequence of typomorphic cumulus assemblages, which, in the first approximation, may be taken for the crystallization sequence of the primary magma.

(4) It was revealed that the complete section of the Layered Series has not been penetrated by boreholes.

(5) It was demonstrated that rocks formed simultaneously in different parts of the magmatic chamber can give diverse geochemical features reflecting the different porosities of cumulus frameworks. This indicates that direct comparison of the chemical characteristics of the rocks of the Aganozero and Burakovo–Shalozero parts of the massif is incorrect.

(6) The peridotite layer complicating the section of the two-pyroxene cumulate zone is morphologically alien to the whole layering of the pluton and may be interpreted as a product of injection of a new magma portion. Because the magma replenishment is an occasional event, the location of the peridotite layer in both blocks within a very narrow interval of the Layered Series is strong evidence for the affiliation of these blocks to a single magmatic chamber.

(7) Leucogabbroids and anorthosites of the zone of two-pyroxene cumulates in the Aganozero block are spatially related to the rocks that experienced strong subsolidus alteration, thus suggesting their possible genetic relations.

ACKNOWLEDGMENTS

We are grateful to the leaders of the Karelian Geological Expedition and its Burakovo Party for giving us the chance to use archive materials. We are grateful to A.A. Ariskin (Vernadsky Institute of Geochemistry and Analytical Chemistry, Russian Academy of Sciences) and A.A. Yaroshevskii (Faculty of Geology, Moscow State University) for helpful advice during preparation of the manuscript.

This study was supported by Sixth Competition–Examination of Young scientists of RAS, 1999 (project no. 300), the Russian Foundation for Basic Research (project nos. 99-05-64875, 99-05-65118, and 01-05-

06271), and the program "Russian Universities" (project no. 015.09.02.016).

REFERENCES

1. Kulikova, V.V., *Volotskaya svita—stratotip nizhnego arkheya Baltiiskogo shchita* (The Volotsk Formation as a Lower Archean Stratotype in Baltic Shield), Petrozavodsk: Karel. Nauchn. Tsentr Ross. Akad. Nauk, 1993.
2. Polikarpov, V.K., Vertical Petrophysical Zoning of the Burakovo Massif (Eastern Onega Area) and Related Anomalies of Physical Fields, in *Petrofizika drevnikh obrazovanii* (The Petrophysics of Ancient Complexes), Apatity, 1986, pp. 45–47.
3. Sobolev, P.O., Deep Structure of the Burakovo Massif, in *Geologiya Severo-Zapada Rossiiskoi Federatsii* (The Geology of Northwestern Russian Federation), Proskuryakov, V.V. and Gaskel'berg, V.G., Eds., St. Petersburg: Severozap. Geol. Tsentr, 1993, pp. 193–207.
4. Garbar, D.I., Sakhnovskaya, T.P., and Chechel', E.K., The Geology and Ore-bearing Potential of the Burakovo–Aganozero Massif, Eastern Onega Area, *Izv. Akad. Nauk SSSR, Ser. Geol.*, 1977, no. 8, pp. 100–112.
5. Lavrov, M.M. and Trofimov, N.N., A New Chromium-bearing Formation in Karelia, in *Rezul'taty polevykh issledovanii 1984 goda. Operativno-informatsionnye materialy* (Results of Field Studies in 1984: On-Line Data), Petrozavodsk: Inst. Geol. Karel. Fil. Akad. Nauk SSSR, 1985, pp. 24–27.
6. Lavrov, M.M. and Trofimov, N.N., The Stratiform Chromite Mineralization of a Layered Intrusion in the Karelian Precambrian, *Dokl. Akad. Nauk SSSR*, 1986, vol. 289, no. 2, pp. 449–451.
7. Goroshko, A.F., Complex Nickel–Magnesia Mineralization in Karelian Ultramafites as a New Geological–Industrial Type of Mineral Deposits, in *Geologiya i poleznye iskopaemye Karelii* (The Geology and Mineral Deposits of Karelia), Golubev, A.I. and Rybakov, S.I., Eds., Petrozavodsk: Karel. Nauchn. Tsentr Ross. Akad. Nauk, 1998, pp. 24–35.
8. Ganin, V.A., Grinevich, N.G., and Loginov, V.N., The Petrology and Ore-bearing Potential of the Burakovo–Aganozero Intrusion, the Eastern Onega Area, in *Platina Rossii* (Platinum of Russia), Moscow: Geoinformmark, 1995, vol. 2, part 2, pp. 19–23.
9. *Metallogeniya Karelii* (The Karelian Metallogeny), Rybakov, S.I. and Golubev, A.I., Eds., Petrozavodsk: Karel. Nauchn. Tsentr Ross. Akad. Nauk, 1999.
10. Pchelintseva, N.F., Nikolaev, G.S., Koptev-Dvornikov, E.V., and Grinevich, N.G., Behavior of Pt, Pd, Au, and Cu during Crystallization of the Burakovo Massif, Southern Karelia, *Dokl. Akad. Nauk,* 2000, vol. 375, no. 4, pp. 521–524.
11. Lavrov, M.M., Olivines and Pyroxenes of the Burakovo Layered Intrusion, in *Mineralogiya magmaticheskikh i metamorficheskikh porod dokeabriya Karelii* (The Mineralogy of Precambrian Igneous and Metamorphic Rocks in Karelia), Petrozavodsk: Inst. Geol. Karel. Nauchn. Tsentr Ross. Akad. Nauk, 1994, pp. 6–41.
12. Koptev-Dvornikov, E.V., Nikolaev, G.S., Ganin, V.A., *et al.*, Vertical Structure of the Aganozero–Burakovo Layered Ore-bearing Intrusion, Southeastern Baltic Shield, *Tezisy dokladov VII Mezhdunarodnogo platinovogo simpoziuma* (Abstracts of Pap. VII Int. Platinum Symp.), Moscow, 1994, p. 48.
13. Nikolaev, G.S., Koptev-Dvornikov, E.V., Ganin, V.A., and Grinevich, N.G., Three-Dimensional Structure of the Burakovo–Aganozero Layered Massif and Distribution of Major Elements in Its Section, *Otech. Geol.,* 1995, no. 10, pp. 56–64.
14. Nikolaev, G.S., Koptev-Dvornikov, E.V., Ganin, V.A., *et al.*, Vertical Structure of the Burakovo–Aganozero Layered Massif and Distribution of Major Elements in Its Section, *Dokl. Ross. Akad. Nauk,* 1996, vol. 347, no. 6, pp. 799–801.
15. Wager, L. and Brown, G., *Layered Igneous Rocks,* Edinburgh: Oliver, 1968. Translated under the title *Rassloennye izverzhennye porody*, Moscow: Mir, 1970.
16. Sharkov, E.V., Bogatikov, O.A., Grokhovskaya, T.L., *et al.*, Petrology and Ni–Cu–Cr–PGE Mineralization of the Largest Mafic Pluton in Europe: The Early Proterozoic Burakovsky Layered Intrusion, Karelia, Russia, *Int. Geol. Rev.*, 1995, vol. 37, pp. 509–525.
17. Snyder, G.A., Higgins, S.J., Taylor, L.A., *et al.*, Archean Enriched Mantle beneath the Baltic Shield: Rare-Earth-Element Evidence from the Burakovsky Layered Intrusion, Southern Karelia, Russia, *Int. Geol. Rev.*, 1996, vol. 38, pp. 389–404.
18. Higgins, S.J., Snyder, G.A., Mitchell, J.N., *et al.*, Petrology of the Early Proterozoic Burakovsky Layered Intrusion, Southern Karelia, Russia: Mineral and Wall-rock Major–Element Chemistry, *Can. J. Earth Sci.*, 1997, vol. 34, pp. 390–406.
19. Chistyakov, A.V., Sukhanov, M.K., Bogatikov, O.A., *et al.*, Distribution of Rare and Rare Earth Elements in the Burakovo Layered Intrusion, Southern Karelia, Russia, *Dokl. Ross. Akad. Nauk*, 1997, vol. 356, no. 3, pp. 376–381.
20. Korneev, S.I., Semenov, V.S., Berkovskii, A.N., *et al.*, The Geology of the Burakovo–Aganozero Layered Intrusion, Southern Karelia, *Tezisy dokladov Mezhdunarodnoi konferentsii "Zakonomernosti evolyutsii zemnoi kory" k 60-letiyu NIIZK* (Abstracts of Pap. Int. Conf. "Regularities of the Earth's Crust Evolution" to 60th Anniv. Res. Inst. Earth's Crust), St. Petersburg: St. Petersburg Gos. Univ, 1996, vol. 2, p. 105.
21. Semenov, V.S., Berkovskii, A.N., Korneyev, S.I., *et al.*, Burakovsky Layered Complex, Karelia: A Multiple Intrusion, *Abstracts of Pap. 30th Int. Geol. Congr., Beijing, China, August 8–14, 1996*, 1996, vol. 2, p. 423.
22. Berkovskii, A.N., Semenov, V.S., Korneev, S.I., *et al.*, The Structure of Burakovo–Aganozero Layered Complex: Petrological Implications, *Petrologiya,* 2000, vol. 8, no. 6, pp. 650–672.
23. Amelin, Yu.V. and Semenov, V.S., Nd and Sr Isotope Geochemistry of Mafic Layered Intrusions in the Eastern Baltic Shield: Implications for the Sources and Contamination of Paleoproterozoic Continental Mafic Magmas, *Contrib. Mineral. Petrol.*, 1996, vol. 124, pp. 255–272.
24. Chistyakov, A.V., Bogatikov, O.A., Grokhovskaya, T.L., *et al.*, The Burakovo Layered Pluton (Southern Karelia) as a Result of in-Space Combination of Two Intrusions: Petrological and Isotope Geochemical Data, *Dokl. Ross. Akad. Nauk*, 2000, vol. 372, no. 2, pp. 228–235.

25. Wright, P.M., Steinberg, E.P., and Glendenin, L.E., Half-Life of Samarium-147, *Phys. Rev.*, 1961, vol. 123, no. 1, pp. 205–208.
26. Donhoffer, D., Bestimmung der Halbwertszeiten der in der Natur Vorkommenden Radioaktiven Nuklide Sm^{147} und Lu^{176} mittels flüssiger Szintillatoren, *Nucl. Phys.*, 1964, vol. 50, no. 3, pp. 489–496.
27. Valli, K., Aaltonen, J., Graeffe, G., *et al.*, Half-Life of Sm-147: Ionization Chamber and Liquid Scintillation Results, *Ann. Acad. Sci. Fenn.*, 1965, ser. A6, issue 177, p. 21.
28. Gupta, M.C. and MacFarlane, R.D., The Natural Alpha Radioactivity of Samarium, *J. Inorg. Nucl. Chem.*, 1970, vol. 32, no. 11, pp. 3425–3432.
29. Lugmair, G.W. and Marti, K., Lunar Initial $^{143}Nd/^{144}Nd$: Differential Evolution of the Lunar Crust and Mantle, *Earth Planet. Sci. Lett.*, 1978, vol. 39, pp. 349–357.
30. Irvine, T.N., Terminology for Layered Intrusions, *J. Petrol.*, 1982, vol. 23, no. 2, pp. 127–162.
31. Ganin, V.A., Loginov, V.N., and Grinevich, N.G., *Geologicheskoe stroenie i poleznye iskopaemye Burakovsko-Aganozerskogo massiva i ego obramleniya. Otchet o rezul'tatakh glubinnogo kartirovaniya masshtaba 1 : 50 000 za 1990–1995 gg.* (Geology and Mineral Deposits of the Burakovo–Aganozero Massif and Adjacent Areas: The Report on Deep Mapping in 1990–1995, Scale 1 : 50000), Petrozavodsk: Karel. Geol. Eksped., 1995.
32. Sharkov, E.V., Bogatikov, O.A., Pchelintseva, N.F., *et al.*, Ore Potential of the Early Proterozoic Burakovo Layered Intrusion, Southern Karelia, in *Platina Rossii* (Platinum of Russia), Moscow: Geoinformmark, 1995, vol. 2, part 2, pp. 10–19.
33. Sobolev, P.O., Orientation of Microscopic Acicular Inclusions of Iron Minerals in Plagioclase: Evidence from the Burakovo Massif, *Zap. Vses. Mineral. O–va*, 1990, vol. CXIX, no. 1, pp. 36–50.
34. Morse, S.A., Kiglapait Geochemistry II: Petrography, *J. Petrol.*, 1979, vol. 20, no. 3, pp. 591–624.
35. Kogarko, L.N., Ni/Co Ratio as an Indicator of Magma Generation in the Mantle, *Geokhimiya,* 1973, no. 10, pp. 1441–1446.